Письма в ЭЧАЯ. 2015. Т. 12, № 1(192). С. 165–170

THE INFLUENCE OF GRAIN BOUNDARIES ON THE LOW-TEMPERATURE THERMAL CONDUCTIVITY OF GRAPHENE NANORIBBONS

D. V. Kolesnikov [1], *V. A. Osipov* [2]

Joint Institute for Nuclear Research, Dubna

The low-temperature thermal conductivity of suspended long and narrow graphene ribbon with domain walls is investigated. Three acoustic phonon branches and the torsion mode are taken into account. The influence of domain walls replaces the low-temperature "quantum-wire" behaviour of thermal conductivity $\kappa \sim T$ with T^n behaviour, where $n < 1$. The transition from "quantum-wire" to "2D graphene"-like behaviour is shifted to the higher temperature when domain walls are present.

В работе исследуется низкотемпературная теплопроводность длинной и узкой свободно подвешенной графеновой полоски в присутствии доменных стенок. Были учтены вклады всех трех акустических фононных мод и моды изгиба. Включение доменных стенок заменяет типичную для квантовой проволоки зависимость теплопроводности от температуры вида $\kappa \sim T$ на T^n, где $n < 1$. Переход от поведения, характерного для квантовой проволоки, к поведению, характерному для двумерного графена, при повышении температуры происходит при большей температуре при наличии доменных стенок.

PACS: 68.35.Ja; 68.65.Pq; 65.80.Ck

INTRODUCTION

Graphene today is known to have remarkable electronic and phononic properties. Certain applications, such as nanoelectromechanical sensors (NEMS) [1] and graphene-based fuel cells [2], require the knowledge of low-temperature characteristics of graphene. In the low-temperature region, the interplay between ballistic transport and diffusive transport due to rough sample borders and polycrystallic structure takes place. The presence of domain walls in graphene and nanoribbons was investigated in several works near room temperature [3–5], and they were shown to have crucial influence on the heat conductivity. Below we will investigate the low-temperature thermal transport properties of graphene nanoribbons in the presence of domain walls.

In Sec. 1, the general formalism for the calculation of thermal conductivity is developed, which takes into account three acoustic phonon branches and ripple torsion mode. The

[1] E-mail: kolesnik@theor.jinr.ru
[2] E-mail: osipov@theor.jinr.ru

dimensionless form for the heat conductivity is calculated, and the effective temperatures for grain boundaries (GB) and rough sample border scattering mechanisms are introduced. In Sec. 2, the heat conductivity is calculated numerically for various grain concentrations and sizes. The role of momentum-dependent rough boundary scattering is discussed in Conclusion. In this section, we also discuss the comparison of thermal conductivity in narrow ribbon with the wide freestanding 2D graphene case.

1. GENERAL FORMALISM

The thermal conductivity of graphene ribbon of length L, width W and effective thickness h_{eff} can be expressed as

$$\kappa = \frac{1}{h_{\text{eff}} LW} \sum_{s,\mathbf{q}} l_s(\mathbf{q}) v_s(\mathbf{q}) \frac{\partial N_0(\omega_s(q))}{\partial T} \hbar \omega_s(q), \tag{1}$$

where $\mathbf{q}$ represents phonon momentum, $l_s(\mathbf{q})$ represents phonon free path for the mode s, $v_s(\mathbf{q})$ is the group velocity for the phonon mode, $\omega_s(q)$ is the phonon dispersion relation, and $N_0(\omega)$ is the Bose–Einstein distribution. For the long and narrow ribbon one can replace the summation over the wider ribbon direction with the integration, so that for the phonon branch s the dispersion relation is $\omega_{n,s} = \omega_s(\sqrt{q^2 + q_n^2})$, $q_n = n\delta q$, $\delta q = \pi/W$, $n = 0, 1, \ldots$, where q is the momentum in the longer direction. We take into account the following phonon modes: the longitudal (LA) and tangential acoustic (TA) modes $\omega_s = v_s q$, $s = \text{LA}, \text{TA}$, the out-of-plane phonon mode (ZA) $\omega_{\text{ZA}} = q^2/(2m)$, $m = 2\sqrt{\rho_{\text{2D}}/K}$, ρ_{2D} is the of graphene 2D mass density and K is the bending stiffness, and the torsion mode $\omega_\tau = v_\tau q$, $v_\tau = \sqrt{8(1-\nu)/(\rho_{\text{2D}} W^2)}$ [8]. Note, that for the torsion mode only $\omega_{\tau,0}$ branch is presented. Introducing the dimensionless parameter $x = \hbar\omega/(k_B T)$, one can find the thermal conductivity in the form

$$\kappa = CT \sum_{s,m} \int_{x_{\min}}^{x_{\max}} \lambda_s(x,T) \frac{x^2 \, \mathrm{e}^x dx}{(\mathrm{e}^x - 1)^2}, \tag{2}$$

where $s = \text{LA}, \text{TA}, \text{ZA}, \tau$,

$$C = \frac{k_B^2 L}{2\pi h_{\text{eff}} W \hbar}, \tag{3}$$

$x_{\max} = \theta_s/T$, $x_{\min} = m\theta_s/T$ for $s = \text{LA}, \text{TA}, \tau$, and $x_{\min} = m^2 \theta_{\text{ZA}}/T$ for ZA branch, $m = 0,\ 1/a_0,\ 2/a_0,\ \ldots (m < W/a_0 - 1)$, a_0 being graphene primitive cell and θ_s being the Debye temperature for the branch s. The relative mean free path $\lambda_s(x,T) = l_s(x,T)/L$ can be expressed as

$$\lambda_s^{-1}(x,T) = 1 + \lambda_{\text{GB}}^{-1} + \lambda_B^{-1}, \tag{4}$$

where 1 stands for ideal ballistic transmission with mean free path L, λ_{GB} represents relative mean free path due to the scattering on the polycrystalline grain boundaries, and λ_B corresponds to the rough borders scattering. The λ_{GB} for LA, TA and torsion mode can be expressed as

$$\lambda_{\text{GB}}(x,T)^{-1} = x \frac{T}{T_{\text{GB}}} \mathcal{G}\left(x \frac{T}{T_0}\right), \tag{5}$$

$s = \mathrm{LA}, \mathrm{TA}, \tau$, $\mathcal{G}(z) = J_0^2(z) + J_1^2(z) - J_0(z)J_1(z)/z$, where $J_n(z)$ is the Bessel function of the 1st kind (see [6]),

$$T_0 = \frac{\hbar v_s}{k_B \mathcal{L}}, \tag{6}$$

and $\mathcal{L}$ being the grain size. The grain boundary effective temperature T_{GB} can be found as

$$T_{\mathrm{GB}} = \frac{\hbar v_s (1 + a/\mathcal{L})^2}{2D^2 \nu^2 k_B L}, \tag{7}$$

where $D = \pi\gamma_s(1 - 2\sigma)/(1 - \sigma)$, γ_s is the Grüneisen constant for branch s and σ is the Poisson constant, ν is the disclination angle in the disclination dipole wall, the average distance between grain boundaries is a, and $(1 + a/\mathcal{L})^{-2}$ is a packing coefficient. Notice that while T_{GB} depends on $a/\mathcal{L}$, T_0 is a function of $\mathcal{L}$ only. For ZA mode with quadratic dispersion relation the grain boundary scattering term in reduced mean free path reads

$$\lambda_{\mathrm{GB}}(x, T)^{-1} = \gamma_{\mathrm{ZA}}^2(x, T) \sqrt{x \frac{T}{T'_{\mathrm{GB}}}} \mathcal{G}\left(\sqrt{x \frac{T}{T_0}}\right), \tag{8}$$

where γ_{ZA} is the momentum-dependent Grüneisen constant for ZA mode, $T_0 = \hbar/(2\mathcal{L}^2 m k_B)$ and

$$T'_{\mathrm{GB}} = \frac{\hbar(1 + a/\mathcal{L})^4}{8 m k_B [D'^2 \nu^2 L]^2}, \tag{9}$$

where $D' = \pi(1 - 2\sigma)/(1 - \sigma)$ (see [5] for detail).

The reduced mean free path due to rough boundary scattering can be expressed as (see [7])

$$\lambda_B(q) = \frac{W(1 + P)}{L(1 - P)}, \tag{10}$$

$P = \exp(-4(q\Delta)^2 \cos\theta_b)$, Δ being mean square deviation of ribbon width and θ_b being angle parameter, varying from $\theta_B = 0$ for armchair borders to $\theta_B = \pi/3$ for zig-zag borders. Expanding the exponent for small Δ, one can find λ_B as

$$\lambda_B(x, T)^{-1} = \left(x \frac{T}{T_B}\right)^2, \tag{11}$$

$$T_B = \frac{\hbar v_s}{k_B \Delta} \sqrt{\frac{W}{2L \cos\theta_b}}. \tag{12}$$

For ZA mode the rough boundary term is the following:

$$\lambda_B(x, T)^{-1} = x \frac{T}{T_b}, \tag{13}$$

where

$$T_b = \frac{\hbar^2}{4 m k_B \Delta^2} \frac{W}{L \cos\theta_b}. \tag{14}$$

2. RESULTS

We have calculated numerically the heat conductivity using Eq. (2) for $W = 2.46$ nm, $L = 1$ μm ribbon.

One can see in the Figure the single-crystal thermal conductivity (dotted curve), and the thermal conductivity in the presence of domain walls (solid and dashed curves, representing $\mathcal{L} = W$ and $\mathcal{L} = W/2$, respectively). One can see that for the defect-free case $\kappa \sim T$ at temperatures below 30 K (quantum-wire behaviour, see [9]), while $\kappa \sim T^{1.5}$ at temperatures above 30 K, which is the well-known low-temperature behaviour of 2D graphene. This behaviour is in good agreement with the elastic-shell-based analytical calculations [8]. On the contrary, the grain boundary scattering leads to the behaviour $\kappa \sim T^n$, where $0.3 < n < 1$, depending on the grain concentration (solid and dashed curves). At the higher temperatures ($T > T_0/2$, see Table 1), the grain boundary scattering leads to the constant mean free path, which results in $\kappa \sim T$ behaviour, and at even higher temperatures — to the normal "2D"- like behaviour. The temperature of transmission from "grain boundary" to "2D" behaviour is determined by two factors: the threshold temperatures $T_0/2$ and the ribbon width W. One can see, that for $\mathcal{L} = W$ these factors are acting simultaneously (solid curves), while for $\mathcal{L} = W/2$ the threshold temperatures are higher and "grain boundary" behaviour continues until higher temperatures (dashed curves).

The influence of rough boundaries with $\Delta \approx 0.1W$ was also calculated. For all the phonon modes T_B was found to be above 70–100 K, so that the influence of edge roughness was found to decrease the power n in T^n behaviour in both polycrystal and single-crystal cases at high temperatures, decreasing with the grain concentration. At the high grain concentrations $a/\mathcal{L} \approx 0$ this influence was found to be negligible. As for the roles of various phonon modes,

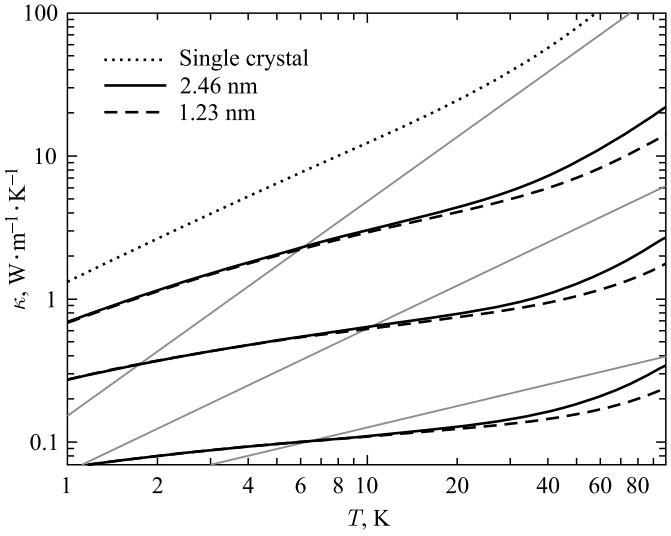

The thermal conductivity vs. temperature for $a/\mathcal{L} = 0.0$, 2.0, 9.0 and $\mathcal{L} = 2.46$ nm (solid curves, from bottom to top) and $\mathcal{L} = 1.23$ nm (dashed curves, from bottom to top). The dotted curve represents defect-free case. The thin lines correspond to the functions $\sqrt{T}, T$ and $T^{3/2}$

Table 1. **The threshold temperature at different grain sizes for three phonon branches**

$\mathcal{L}$, nm	T_0, K (LA)	T_0, K (TA)	T_0, K (ZA)	T_0, K (τ)
1.23	132.0	84.2	1.2	3.66
2.46	66.0	42.1	0.6	1.83

Table 2. **The grain boundary temperature at different effective distances between grains for the case of high-angle grain boundaries ($\nu = 1/12$)**

$a/\mathcal{L}$	T_{GB}, mK (LA)	T_{GB}, mK (TA)	T'_{GB}, mK (ZA)	T_{GB}, mK (τ)
0.0	15	55	$1.3 \cdot 10^{-6}$	0.03
2.0	135	495	$1.06 \cdot 10^{-4}$	0.25
9.0	1497	5506	0.013	2.77

the ZA mode was found to dominate other modes for the single-crystal case only. The presence of grain boundaries gave rise to the deformation potential-type scattering, leading to the suppression of ZA mode due to the high momentum-dependent Grüneisen constant even at low reduced grain concentration ($a/\mathcal{L} \approx 10$). The LA and TA modes were found to have effectively equal influence on the thermal conductivity, while the low-energy torsion mode plays role at low temperatures only.

CONCLUSION

In conclusion, we have investigated the influence of grain boundaries on the heat conductivity of graphene ribbons. Similar to the case of 2D graphene samples, the power in the power-law dependence of thermal conductivity on temperature is reduced due to the presence of domain walls (cf. [5]). At higher temperatures the grain boundary scattering results in constant mean free path and reducing the role of flexural ZA phonon mode, reducing the magnitude of heat conductivity and leaving the power-law temperature dependence intact. The difference between the 2D graphene and ribbon cases is the presence of one-dimensional quantum-wire behaviour at the temperatures below the geometry-driven threshold temperature. When grain boundaries are presented, this behaviour is also modified below the GB threshold temperature, and this temperature is always equal to or higher than the temperature modification due to ribbon width (quantum-wire threshold). The reason for the relation between temperatures is geometrical: both the GB threshold and the quantum-wire threshold temperatures are dependent on the effective size (the grain size and the ribbon width, respectively), and the size of the grain is naturally limited with the lowest size of the sample.

This work has been supported by the Russian Foundation for Basic Research under grant No. 12-02-01081.

REFERENCES

1. *Singh V. et al.* // Nanotechnology. 2010. V. 21. P. 165204.
2. *Antolini E.* // Appl. Catalysis B: Environmental. 2009. V. 88. P. 24.

3. *Neek-Amal M., Peeters F. M.* Effect of Grain Boundary on the Buckling of Graphene Nanoribbons // Appl. Phys. Lett. 2012. V. 100. P. 101905.
4. *Nika D. L., Balandin A. A.* Phonon Transport in Graphene // J. Phys.: Condens. Matter. 2012. V. 24. P. 233203.
5. *Kolesnikov D. V., Osipov V. A.* // Europhys. Lett. 2012. V. 100. P. 26004.
6. *Krasavin S. E., Osipov V. A.* // J. Phys.: Condens. Matter. 2001. V. 13. P. 1023.
7. *Askamija Z., Knezevic I.* // Appl. Phys. Lett. 2011. V. 98. P. 141919.
8. *Munos E., Lu J., Yakobson B.* // NANO Lett. 2010. V. 10. P. 1652.
9. *Rego L. G. C., Kirczenow G.* // Phys. Rev. Lett. 1998. V. 81. P. 232.

Received on April 28, 2014.